Textures and Microstructures, 1995, Vol. 26–27, pp. 103–110
Reprints available directly from the publisher.
Photocopying permitted by license only

THE MODIFIED MAXIMUM ENTROPY METHOD (MMEM) IN QTA FOR LOWER SYMMETRY POLYCRYSTALLINE AGGREGATES

Y. D. WANG, J. Z. XU and Z. D. LIANG

Dept. of Materials Science & Engineering, Northeastern University, Shenyang 110006, People's Republic of China

(Received 2 October 1995)

A new algorithm of quantitative texture analysis (QTA), which is called the modified maximum entropy method (MMEM), has been proposed and applied to determination of textures in polycrystalline samples of lower crystal symmetry with overlapping diffraction peaks (Wang and Xu, 1995a). By introducing directly the maximum entropy principle into the least square procedure of pole figure inversion (Bunge, 1969), then both minimizing the differences between experimental and postulated pole figure data, and maximizing entropy may be satisfied simultaneously. Thus, the maximum entropy principle is applied to the entire process of QTA in frame of the harmonic method (HM). The detailed comparisons among the three pole figure inversion methods, i.e. the traditional HM, the primary maximum entropy method (MEM) and the MMEM, are given through a model example of simulated fiber texture. It is shown that the precise and stable solution of inverse pole figure for the polycrystalline samples with smooth or sharp textures will be obtained by the MMEM even using a less number of pole figures. The minimum range of polar angle and the least number of pole figures, which are needed in the QTA for pretended tetragonal materials by the MMEM, are discussed in detail.

KEY WORDS: Texture quantitative analysis, modified maximum entropy method, lower crystal symmetry, overlapping peaks.

INTRODUCTION

As there has been of great interest in some advanced materials such as intermetallics, ceramics, polymers and geological materials, much efforts were made to overcome the difficulties in quantitative texture analysis (QTA) for the lower symmetry polycrystalline samples with overlapping diffraction peaks. So far, many methods such as the iterative positive method (Dahms and Bunge, 1988), the vector method (Ruer and Baro, 1977; Vadon, 1981), the component method (Helming, 1991) and the WIMV (Matthies and Vinel, 1982; Kallend, Schwarz and Rollett, 1991) have been applied to the QTA for the lower symmetry crystallites with single or/and overlapping diffraction peaks. The concept of 'maximum entropy', which has been widely accepted in the information theory and the image reconstruction, was introduced to QTA for cubic and hexagonal materials with series coefficients as restrictive conditions (Wang, Xu and Liang, 1987, 1989), i.e. the maximum entropy method (MEM). Quite recently, it has been applied to determining the fiber texture vector of tetragonal materials with overlapping Bragg-diffraction (Wang, Xu, 1995b). In the MEM, while the positivity condition of ODF is automatically satisfied, the assumption of maximum entropy may give an access, with less number of pole figures, to the optimization of pole figure inversion within

the variation width of solution. However for tetragonal materials a fair solution may be obtained by the MEM even from less number of pole figures merely in the case of smooth texture. If the texture is very sharp, because of the less number of pole figures used, the lack of enough ODF coefficients as constraints would lead to an unstable solutions with larger errors in the QTA.

The MMEM, which introduces maximum entropy principle directly into the least square equation of pole figure inversion proposed by Bunge (1969), may overcome the drawback of the QTA by the primary MEM. It has been proved that the satisfactory results could be got by the MMEM even from less pole figure data. In present paper, the minimum range of polar angle and the least number of measured pole figure data which are needed in QTA for tetragonal materials by the MMEM are also discussed through the inverse pole figure analysis.

MAXIMUM ENTROPY PRINCIPLE IN QTA

The MEM with series coefficients W_{lmn} as constraints

The series coefficients W_{lmn} and normalized factor N_{cj} of the jth single lattice plane of the Cth measured pole figure can be solved by using least square method from overlapping pole figures (Wang, Xu, 1995b), i.e.

$$\sum_{c=1}^{S} \iint_{\Omega} [q_c(\chi,\eta) - \sum_{j=1}^{J} N_{cj} \sum_{l=0}^{L} \sum_{m=-l}^{l} \sum_{n=-l}^{l} 2\pi(\frac{2}{2l+1})^{1/2} W_{lmn} P_l^m(\cos\chi) e^{-im\eta} P_l^n(\cos\Theta_{cj}) e^{in\Phi_{cj}}]^2 \sin\chi d\chi d\eta = \min \quad (1)$$

Where S and Ω are the number and the range of measured pole figures, respectively; $q_c(\chi,\eta)$ is the pole density of the Cth measured pole figure; $p_l^m(\cos\chi)$, $p_l^n(\cos\Theta_{cj})$ are the normalized Legendre polynomials; Θ_{cj}, Φ_{cj} are the spherical polar coordinates of the jth single lattice plane of the Cth measured pole figure.

Following the MEM proposed by Wang, Xu, Liang, (1987, 1989), the restrictive conditions can be written as

$$W_{l'm'n'} = \sum_{k=1}^{K} \sigma^k_{l'm'n'} \exp(-1-\lambda_0 - \sum_{l=1}^{L} \sum_{m=-l}^{l} \sum_{n=-l}^{l} \lambda_{lmn} \sigma^k_{lmn}) \quad (2)$$

with

$$K = \sum_{k=1}^{K} \exp(-1-\lambda_0 - \sum_{l=1}^{L} \sum_{m=-l}^{l} \sum_{n=-l}^{l} \lambda_{lmn} \sigma^k_{lmn}) \quad (3)$$

and the texture vector Y_k can be expressed by following Eq.

$$Y_k = \exp(-1-\lambda_0 - \sum_{l=1}^{L} \sum_{m=-l}^{l} \sum_{n=-l}^{l} \lambda_{lmn} \sigma^k_{lmn}) \quad (4)$$

Where σ^k_{lmn} is the matrix connecting the texture vector and the series coefficients W_{lmn}; K is the total number of vector boxes as defined by the VM (Ruer and Baro, 1977); λ_0 and λ_{lmn} are the unknown Lagrangian multipliers.

In primary MEM, it was suggested to proceed as follows: calculate texture coefficients W_{lmn} from Eq. (1), then calculate texture vector Y_k by solving the non-linear Eqs. (2) with the restrictive condition (3). For the samples with smooth textures or enough number of measured pole figures used as input data, the precise texture vector may be provided by the MEM. However, according to the algorithm described above, the maximum entropy optimum is only entered into the second stage in texture analysis (Schaeben, 1991). Thus, if less number of pole figures were used as the input data of QTA, especially for the lower symmetry crystalline aggregates with extremely sharp texture components, the texture coefficients obtained would be too few to get a fair solution.

The MMEM with pole figure data as constraints

According to the MMEM, Eqs. (4) are directly introduced into Eq. (1)

$$\sum_{c=1}^{S} \iint_{\Omega} [q_c(\chi, \eta) - \sum_{j=1}^{J} N_{cj} \sum_{l'=0}^{L'} \sum_{m'=-l'}^{l'} \sum_{n'=-l'}^{l'} 2\pi(\frac{2}{2l'+1})^{1/2}$$

$$P_{l'}^{m'}(\cos\chi)e^{-im'\eta}P_{l'}^{n'}(\cos\Theta_{cj})e^{in'\Phi_{cj}} \sum_{k=1}^{K} \sigma^{K}_{l'm'n'}$$

$$\exp(-1-\lambda_0 - \sum_{l=1}^{L} \sum_{m=-l}^{l} \sum_{n=-l}^{l} \lambda_{lmn}\sigma^{K}_{lmn})]^2 \sin\chi d\chi d\eta = \min \qquad (5)$$

There, L is the order of the series expansion in orientation space which should correspond to the total number of measured pole figures; L' is the order of the series expansion of pole figure inversion which may be extended to a larger value according to the texture index of measured materials. If L' $\rightarrow \infty$, the pole figure inversion should be replaced by the matrix in the VM. In this paper, for tetragonal materials, L' and L are 22 and 10 respectively.

It is shown that the new algorithm introduces maximum entropy principle directly into the least square procedure of pole figure inversion in frame of the HM. Thus, it can be applied to the entire processes of the QTA.

In the case of fiber texture, Eq. (5) reduces to

$$\sum_{c=1}^{S} \int_{\Omega} [q_c(\chi) - \sum_{j=1}^{J} N_{cj} \sum_{l'=0}^{L'} \sum_{n'=-l'}^{l'} 2\pi(\frac{2}{2l'+1})^{1/2} P_{l'}(\cos\chi)$$

$$P_{l'}^{n'}(\cos\Theta_{cj})e^{-in'\Phi_{cj}} \sum_{k=1}^{K} \sigma^{K}_{l'n'} \exp(-1-\lambda_0 - \sum_{l=1}^{L} \sum_{n=-l}^{l} \lambda_{ln}\sigma^{K}_{ln})]^2 \sin\chi d\chi = \min \qquad (6)$$

where $q_c(\chi)$ is the axial density of the Cth measured pole figure. The fiber texture analysis is important not only to the samples with rotational texture, but also to the verification of the MMEM suiting for materials with arbitrary textures.

EXAMPLES OF FIBER TEXTURE ANALYSIS

Methodology Comparisons

Three methods, i.e. the MMEM, the MEM and the traditional HM, are compared through model function of fiber texture of tetragonal materials (Assuming c/a = 1.02) with single

or/and overlapping diffraction peaks. The ideal fiber textures are given in Gauss distribution. The axial intensity S is described by

$$S(\omega) = B_0 + \sum_i s(\omega_i) \exp\left\{-\frac{(\omega - \omega_i)^2}{\psi_i^2}\right\} \tag{7}$$

where ω_i is the orientation of fiber i in the crystallographic space; ψ_i its standard scatter (half) width of the Gauss distribution and B_0 the background. Five pretended axial pole figure with single or overlapping reflections, i.e. (110), (111), (002) + (200), (112) + (211), and (131) + (113), are pre-determined by the HM ($L_{max} = 22$).

Firstly, the smoother texture with two components, (111) and (110) ($\psi_i = 14°$), and 10% background are assumed (Figure 1(a)) (Wang and Xu, 1995b). Figure 1(b) gives the inverse pole figures derived by the traditional HM from above five incomplete pole density curves ($\chi_i = 70°$). It can be seen that some negative regions and 'ghost' peaks are present there and all the peaks are lowered as compared to the original. Figure 1(c) (d) give the inverse pole figures derived by the MEM and the MMEM, respectively, from the same number of incomplete pole densities. Here negative regions and 'ghost' peaks disappear and the peak intensities are considerably increased. Obviously, introduction of maximum entropy principle into the QTA overcomes the serious series truncation of the traditional HM.

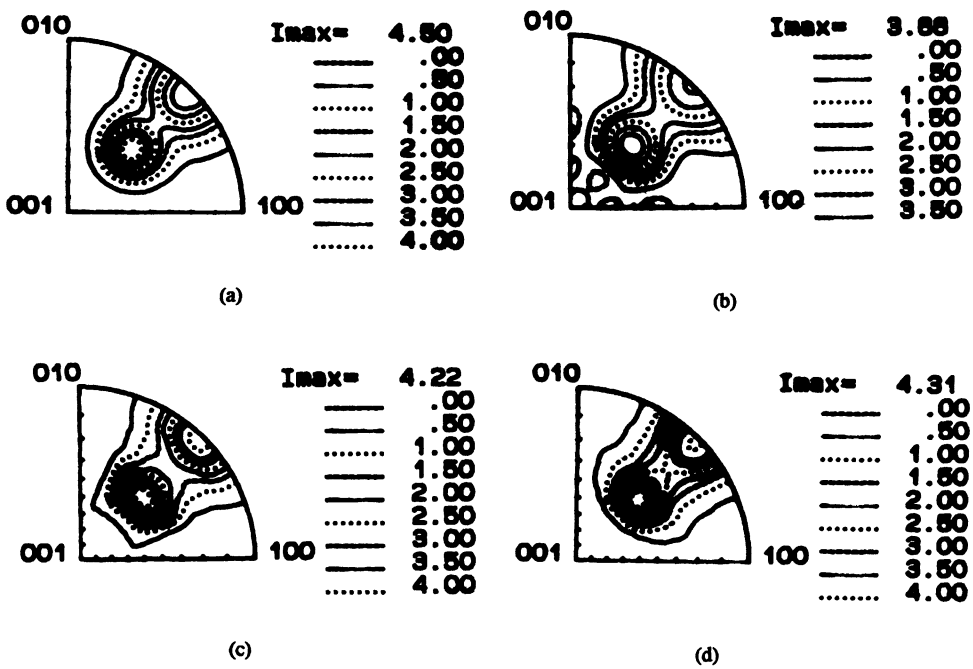

Figure 1 The inverse pole figure (a) assumed with (111) and (110) components in Gauss distribution ($\psi_i = 14°$ and 10% background) and calculated by (b) the traditional HM, (c) the MEM (Wang, Xu, 1995b) and (d) the MMEM from the five incomplete pole densities ($\chi_i = 70°$), i.e. (110), (111), (002) + (200), (220) + (022) and (311) + (113).

Secondly, the sharper texture with the same components with scatter width of 10° and 10% background are assumed (Figure 2(a)) (Wang and Xu, 1995a). Figure 2(b)(c) give the inverse pole figures determined by the traditional HM, the MEM respectively. Similarly to those in Figure 1(b), considerable negative intensities and 'ghost' peaks are also shown in the inverse pole figure derived by the traditional HM. In spite of no more negative regions in the inverse pole figure recalculated by the MEM, the 'ghost' peaks still remain a little and, compared to the original, the extremely higher value and the distorted shape of the peaks are illustrated. However, the precise inverse pole figure is reproduced by the MMEM (Figure 2(d)). The negative regions and 'ghost' peaks disappear and the peak intensities are close to the assumed value.

Figure 3 gives the postulated and recalculated pole densities as a function of tilt angle for (110) and (200) + (002) pole respectively. It is shown that the pole densities recalculated by the MMEM, for both (110) and (200) + (002) poles, agree well with the postulated value. However, the recalculated value by the MEM shows obvious difference from the postulated, especially for superimposed pole densities (Figure 3(b)). Therefore, the MMEM shows great advantage over the primary MEM in the QTA for the polycrystalline samples of low symmetry with overlapping diffraction peaks.

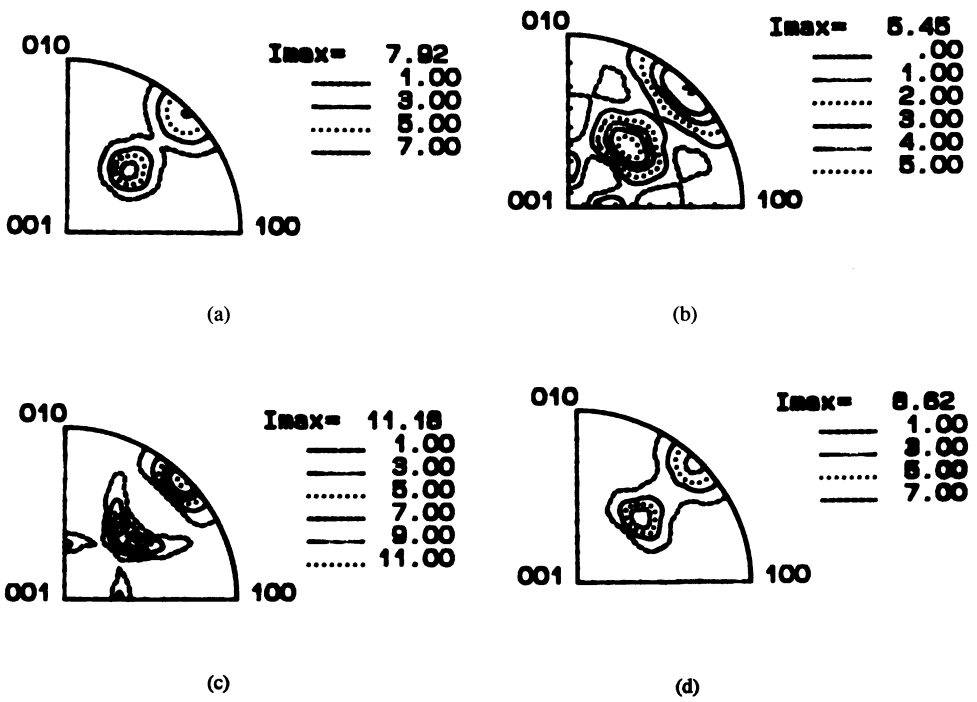

Figure 2 The inverse pole figure (a) assumed with (111) and (110) components in Gauss distribution (ψ_i = 10° and 10% background) and calculated by (b) the traditional HM, (c) the MEM (Wang, Xu, 1995b) and (d) the MMEM from the five incomplete pole densities (χ_i = 70°), i.e. (110), (111), (002) + (200), (220) + (022) and (311) + (113) (Wang, Xu, 1995a).

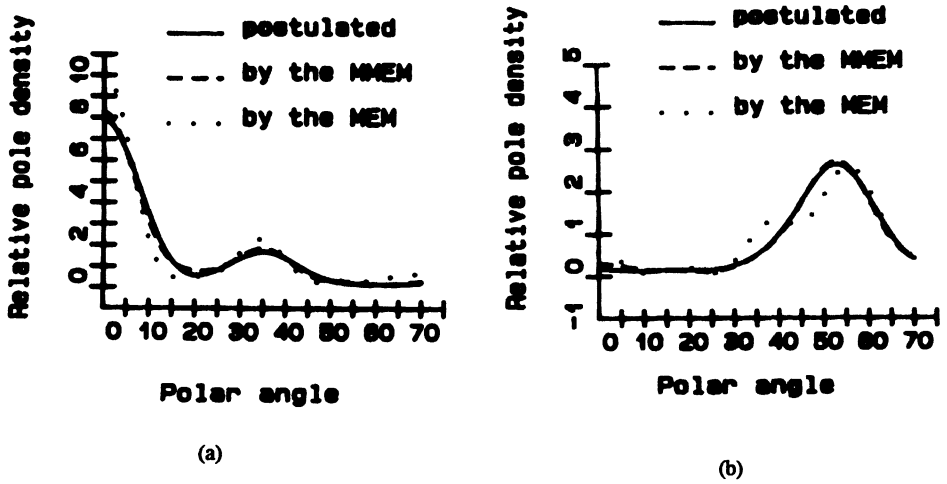

Figure 3 The postulated and recalculated pole densities as a function of tilt angle for (a) (110) (b) (200) + (002) poles (Wang, Xu, 1995a).

The range of polar angle and the least number of pole figures for fiber texture analysis by the MMEM

The assumed inverse pole figure with three components, (111), (110) and (100) ($\psi_i = 10°$), and 10% background is shown in Figure 4(a). Figure 4(b)(c) give the inverse pole figures recalculated by the MMEM from five pole densities described above with $\chi_f = 90°$ and 70° respectively. It can be seen that the precise inverse pole figure may be obtained from the input data $\chi_f \geq 70°$. However, if incomplete pole figures ($\chi_f = 50°$) are used as input data, the 'ghost' peak with (001) component appears in the recalculated inverse pole figure, which indicates that it is not possible to derive the inverse pole figure from the five incomplete pole figures ($\chi_f \leq 50°$) by the MMEM in present assumed textures. In fact, if another constraints are introduced into the QTA, the range of polar angle or the input data may be further reduced.

Figure 5(a) gives the inverse pole figure recalculated from four incomplete pole density curves, i.e. (110), (111), (002) + (200) and (220) + (202) ($\chi_f = 70°$), which almost the same as that recalculated from five incomplete curves. The precise inverse pole figure (Figure 5(b)) can be derived even from only one (110) incomplete pole density ($\chi_f = 70°$), which indicates that the MMEM may obviously reduce the pole figure data in the QTA for lower symmetry polycrystalline aggregates.

Figure 6 gives the inverse pole figure recalculated from one superimposed pole density curve (113) + (311) with $\chi_f = 90°$ and 80° respectively. It is shown that more precise inverse pole figure may be obtained only from complete pole density ($\chi_f = 90°$) (Figure 6 (a)). However, as the range of polar angle decreases, the lost information leads to the unstable solution of inverse pole figure (Figure 6(b)). Thus, it may be drawn that, compared to the single pole figure, the superposed pole figure provides less information in the QTA.

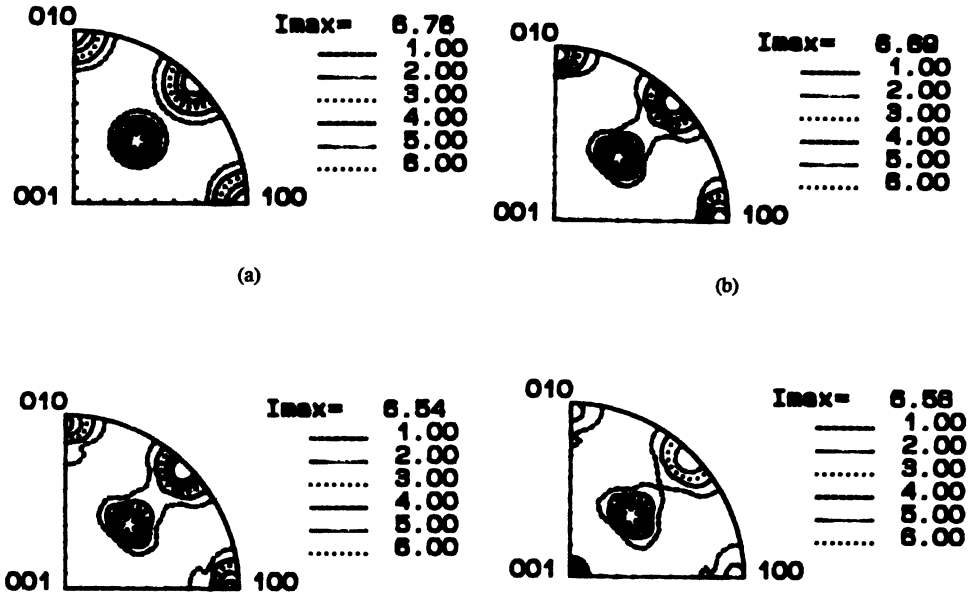

Figure 4 The inverse pole figure (a) assumed with (111), (001) and (110) components in Gauss distribution (ψ_i = 10° and 10% background) and calculated by the MMEM from the five pole figures (b) (χ_f = 90°), (c) (χ_f = 70°) and (d) (χ_f = 50°), i.e. (110), (111), (002) + (200), (220) + (022) and (311) + (113).

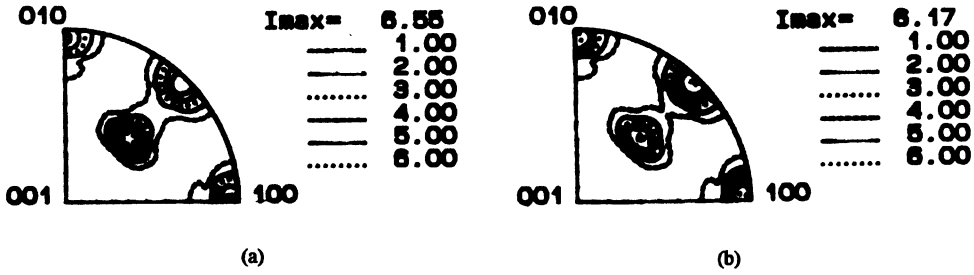

Figure 5 The inverse pole figure calculated by the MMEM from (a) the four pole density curves, i.e. (110), (111), (002) + (200), (220) + (022), and (b) (110) pole density curve (χ_f = 70°) only.

CONCLUDING REMARKS

The MMEM has been proposed and successfully applied to the QTA for lower symmetry polycrystalline aggregates with single or/and superposed pole figures. Thus, we apply the maximum entropy principle to the entire process of QTA in frame of the HM.

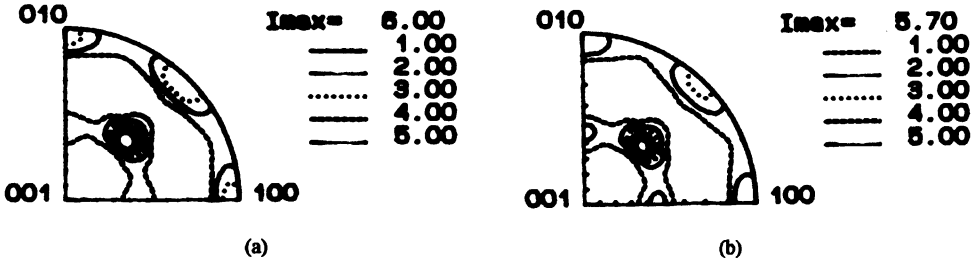

Figure 6 The inverse pole figure calculated by the MMEm from only (113) + (311) superimposed pole figures with various range of polar angles. (a) (χ_f = 90°) and (b) (χ_f = 80°).

Compared to the primary MEM, the less pole figure data are needed to obtain a stable solution in the QTA by the algorithm described above. It is also shown that, compared to the single pole figure, the superposed pole figure provides less information in orientation analysis.

Acknowledgements

The authors wish to acknowledge Prof. L. Zuo for his helpful discussions in this study. This work was supported by the National Natural Science Foundation of China.

References

Bunge, H. J. (1969). Mathematische Methoden der Texturanalyse, Akademie-Verlag: Berlin (DDR).
Dahms, M. and Bunge H. J. (1988). *Textures and Microstructures*, **10**, 21.
Helming, K. (1991). *Textures and Microstructures*, **14–18**, 187.
Kallend, J. S., Schwarz, R. B. and Rollett, A. D. (1991), *Textures and Microstructures*, **13**, 189.
Matthies, S. and Vinel, G. W. (1982). Physical Statuts Solidi (b), **112**, k111.
Reur, D. and Baro, R. (1977). Advance of X-ray Analysis, **20**, 187.
Schaben, H. (1991). Journal of Applied Physics, **69**(3), 1320.
Vadon, A. (1981). Generalisation et Optimiseation de la Methode Vectorielle d'Analyse de la Texture, These, University of Metz, France.
Wang, F., Xu, J. Z. and Liang, Z. D. (1987). Eighth International Conference on Textures of Materials (ICOTOM8), J. S. Kallend and G. Gottstein eds., The Metallurgical Society, Inc., Santa Fe, USA, 801.
Wang, F., Xu, J. Z. and Liang Z. D. (1989). *Textures and Microstructure*, **10**, 217.
Wang, Y. D. and Xu, J. Z. (1995a). Quantitative Texture Analysis for the Lower Crystal Symmetry Polycrystalline Materials with Overlapping Diffraction Peaks. Acta Metallurgica Sinica (Chinese Edition), **31**, (in press).
Wang, Y. D. and Xu, J. Z. (1995b). Determination of Fiber Texture Vector from Overlapping Pole Figures by the Maximum Entropy Method, Scripta Metallurgica et Materials, **33**, 1049.